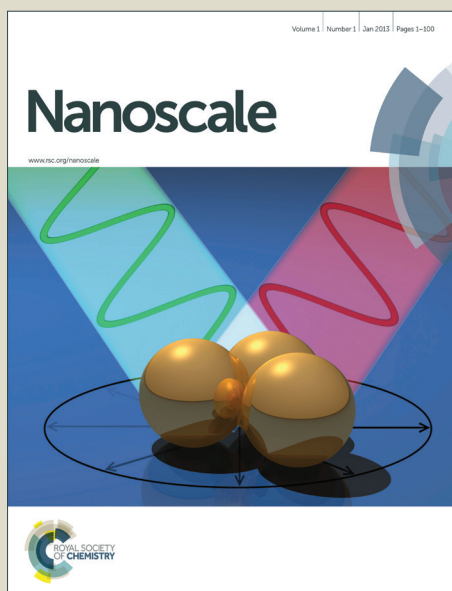


Nanoscale

Accepted Manuscript



This is an *Accepted Manuscript*, which has been through the Royal Society of Chemistry peer review process and has been accepted for publication.

Accepted Manuscripts are published online shortly after acceptance, before technical editing, formatting and proof reading. Using this free service, authors can make their results available to the community, in citable form, before we publish the edited article. We will replace this *Accepted Manuscript* with the edited and formatted *Advance Article* as soon as it is available.

You can find more information about *Accepted Manuscripts* in the [Information for Authors](#).

Please note that technical editing may introduce minor changes to the text and/or graphics, which may alter content. The journal's standard [Terms & Conditions](#) and the [Ethical guidelines](#) still apply. In no event shall the Royal Society of Chemistry be held responsible for any errors or omissions in this *Accepted Manuscript* or any consequences arising from the use of any information it contains.

Advanced nanoarchitectures of silver/silver compound composites for photochemical reactions

Mingce Long, Weimin Cai*

School of Environmental Science and Engineering, Shanghai Jiao Tong University, Dongchuan

Road 800, Shanghai 200240, China

* Corresponding author:

Tel.: +86-21-54747354;

Fax: +86-21-54740825.

E-mail address: wmcai@sjtu.edu.cn (W.M. Cai)

Postal address:

School of Environmental Science and Engineering, Shanghai Jiao Tong University, Dongchuan

Road 800, Shanghai 200240, China

Abstract

Silver/silver compound (SSC) composites have received much attention as a type of potential materials in photochemical reactions due to their high efficiency, facile syntheses and availability of raw materials. This article reviews the state-of-the-art progresses on the advanced nanoarchitectural SSC composites. We begin with a survey on the general synthetic strategies for SSC composites, and then step into relatively detailed methods for sizes and morphologies tunable two-component and more delicate multi-component SSC nanostructures. In addition, the electronic structure relevant mechanisms of such materials and the recent studies on their stability have been summarized. This review also highlights some perspectives on challenges related to the SSC composites and the possible researches in the future.

1. Introduction

Photochemical conversion of solar energy has found broad potential applications, including photocatalytic pollutant removal, photocurrent generation, water splitting, solar cells, sensors, and so on.¹⁻⁴ Recently with the increasing attention on artificial photosynthesis and clean hydrogen energy from water and sunlight, nanomaterials with the ability to initiate or promote photochemical reactions have been extensively studied.^{4,5} Although remarkable progress has been achieved in both the synthetic strategy for advanced nanostructures and the basis of photochemical mechanism, it is still a big challenge to realize practical applicable efficiency for photo-electrical conversion of natural sunlight. Much more efforts are still required to understand the primary interaction processes of photons and electrons in the related nanomaterials, and the basic laws on the relationship between the microstructures of materials and their photo-responsive behaviors.

Fabricating advanced nanoarchitectures is regarded as a crucial approach to obtain materials with improved efficiency and stability in photochemical reactions.^{4,6} In the latest years, silver/silver compound (SSC) composites become to be one type of attractive materials, due to the merits including the high efficiency in photochemical reactions, facile syntheses and availability of raw materials. In fact, most silver compounds possess unique properties including light sensitivity, electrical and ionic transport behavior, semiconductor features, and so on. All of these properties enable them being applied for decades in such fields as electrodes, infrared spectroscopy, radiometry, and heterodyne detection. Even more, silver halide AgX (X=Cl, Br, I) have been utilized in photography for over a century, due to the well-known photochemical transformation of AgX, occurring when exposed to even red light, named as Herschel effect. However, the study of silver compounds in the field of photochemical water splitting is initiated only very recently. In 1999, the pioneer work was done by Ashokkumar et al., who studied the water splitting by Ag and AgCl colloid, and proposed a redox reaction cycle of AgCl-Ag-AgI system.⁷ In the same year, Kakuta and Calzaferri's group investigated the water splitting over AgBr/SiO₂⁸ and the photoelectrochemical behavior of a AgCl electrode,⁹ respectively. With the improvement of synthetic methods, SSC composites with diverse advanced nanostructures were fabricated. It was found that under illumination of visible light, the SSC composites display efficient activity for organic degradation,¹⁰⁻¹⁵ antibacterial¹⁶⁻¹⁸, water splitting¹⁹⁻²² and CO₂ reduction^{23,24}, which stimulated great

efforts on such materials, especially on the fabrication of advanced nanostructures with improved performance in photochemical reaction. This review aims to provide a relatively overall and updated summary of the current progress on this type of SSC composites. It will start from the general strategies for the syntheses of SSC composites, and then followed with the methods to assemble size and morphology tunable nanostructures of two-component SSC (TSSC) and more delicate nanoarchitectures of multi-component SSC (MSSC) composites. We will also give an overview on the latest results on the electronic structure related mechanisms, and discussed the photochemical stability of this type of nano-composites. Finally, some challenges confronted on the SSC composites in photochemical reactions will be discussed in the conclusion and outlook section. By this comprehensive review, we hope to provide implications for the development of highly efficient and stable SSC materials for the applications of photochemical reactions, as well as to advance further exploration on the controllable mechanisms and novel strategies for chemical conversion of light energy with new materials.

Before this review, two things should be specially noted. Firstly, SSC composites in this review include all kinds of contact forms, such as encapsulated core-shell (silver could be core or shell), heterojunction, embedment, isolation, and other more complicated forms for MSSC. For more concise, in most cases we use silver/silver compound for all contact form, even for the core-shell structure that is frequently reported as silver@silver compound or silver compound@ silver. Secondly, although there are some reports on the exclusive silver compounds and their photocatalytic performance, silver nanoparticles would form more or less over the surface and result in a SSC structure when upon illumination due to their light sensitivity and self-decomposition behavior. Therefore we would like to include these references in this review. The basic information of some typical silver compounds is shown in Table 1.

Table 1 Basic information of typical silver compounds

(X, Absolute Electronegativity; CB, conduction band)

Compounds	Band gap (eV)	Crystal structure	X	Estimated CB (eV)
Ag₂O	1.20 ²⁵	Cubic (Pm3m)	5.30	+0.2*/+0.2 ²⁵
AgCl	3.25 ²⁶	Cubic (Fm3m)	6.07	-0.05*
AgBr	2.60 ²⁶	Cubic (Fm3m)	5.81	0.01*
AgI	2.86 ²⁷	γ phase: Cubic (F-43m) β phase: Hexagonal (P63mc)	5.49	-0.45*
Ag₂S	2.30 ²⁸	Cubic (Im3m)	4.97	-0.68*/-0.82 ²⁹
Ag₃PO₄	2.36 ³⁰	Cubic (P-43m)	5.96	+0.28*
Ag₂CO₃	2.30 ³¹	Monoclinic (P21)	6.13	+0.48*/+0.37 ³¹
Ag₂CrO₄	1.75 ³²	Orthorhombic (Pnma)	5.86	0.48*
Ag₂MoO₄	3.37 ³³	Cubic (Fd3m)	5.90	-0.29*
Ag₃VO₄	2.16 ³⁴	Monoclinic (C2/C)	5.64	0.06*
Ag₂SiO₃	2.60 ²⁰	Orthorhombic (P212121)	5.86	0.06*

*: estimated according to Equation 3. See section 3.2.

2. Synthesis and assembly

Normally, there are three strategies for the syntheses of SSC composites. (1) Reduction process: partially reducing the previous synthesized silver compounds to Ag⁰ nanoparticles by the addition of chemical reductant (CR), photo-irradiation reduction (PIR) or polyol-assisted reduction (PAR). In these reduction approaches, PIR is the most frequently used method, because it is possible to form a core-shell nanostructure with Ag⁰ generated over the surface layer via a facile operation; CR is not flexible for morphology control, but has a lot of choices on the reductants, such as NaBH₄,³⁵ L-arginine^{36,37} and beet juice;³⁸ PAR is a general method to synthesize nanostructural Ag⁰, which can be applied accompanying with the preparation of AgX in the polyol solution,³⁹ or as a separated process for the reduction of any silver compounds.^{40,41} (2) Oxidation process: performing a chemical transformation to form silver compounds from the Ag⁰ precursor. In this method, the oxidation of Ag⁰ and the generation of silver compounds are simultaneously achieved by selecting proper

oxidizing reagents based on their redox potentials.⁴² (3) One pot method: simultaneously generate the composites of silver and silver compounds in a mixture with a certain reducing ability. The reducing ability could be generated by external energy inputs such as microwave,⁴³ sonication⁴⁴ or by choosing proper additives, such as pyridine⁴⁵ or ionic liquids,⁴⁶ which having mild reducing ability at (hydro/solvo)thermal conditions.

2.1 Two-component SSC (TSSC) composites

Ag/AgX (X=Cl, Br and I) must be one of the mostly investigated SSC composites due to their exceptional high photocatalytic activities. Synthesis of AgX nanoparticles is the prerequisite step in the reduction or one pot strategies. Although AgX compounds can be directly prepared by precipitation from Ag⁺ and X⁻ ions in aqueous solution because of their low solubility (AgCl: 1.9×10^{-3} , AgBr: 1.4×10^{-4} and AgI: 3.1×10^{-5} g L⁻¹ at 25 °C), it is still a big challenge to obtain size and morphology controllable AgX nanoparticles since the precipitation reaction is very fast. A few approaches have been developed to slow down the reaction and regulate the nanostructure of AgX, including the addition of surfactants, the replacement of reaction medium with high viscosity liquid, such as EG or ionic liquid, and the selection of proper reactant.

Surfactants, such as poly (vinyl alcohol) PVA^{36,47} and poly (vinyl pyrrolidone) (PVP),^{39,48} are served as dispersing agents, stabilizers or templates to inhibit agglomeration and assist the nanocrystal oriental growth. With the assistant of PVA, 20 nm AgCl nanoparticles with a good dispersion has been obtained by Choi's group.⁴⁷ In addition, surfactants with halogen anions could be used as both surfactant and reactant. For example, cetyltrimethylammonium chloride (CTAC),⁴⁹ hexadecyltrimethylammonium bromide (CTAB)^{23,50-53} and tetra-octylammonium bromide (TAOB)⁵⁴ have been used as Cl and Br sources for the corresponding AgX nanoparticles. Micelles formed from the aggregation of surfactant molecules are commonly employed to synthesize nanomaterials. By fabricating the micelle and regulating the ratio of oil and water, morphology controllable Ag/AgX nanocomposites can be obtained. An et al. developed a reverse micelle method to synthesize AgCl nanocubes by using NaCl and AgNO₃ as the precursors, and employing PVP and P-tolyl sulfonic acid to form reverse micelle.³⁵ The average edge length of as-prepared AgCl is 85 nm, which was partially reduced by NaBH₄ to form Ag/AgCl nanocomposite. Oil-in-water⁵¹ or water-in-oil⁵⁵ system has been realized by mixing the CTAC chloroform solution and AgNO₃ aqueous solution. By tuning the ratio of the oil and water solution and the concentration of CTAC, spherical or cubic Ag/AgCl

nanostructures were produced without further post treatments. In addition, Dong et al. proposed a method to synthesize well defined cubic Ag/AgCl by adding gelatin and precisely controlling a relatively low and constant concentration of $[Cl^-]$, in which gelatin serves as capping agent to promote the orientation growth and restrain the aggregation of AgCl grains.⁵⁶

Ethylene glycol (EG) is employed as the solvent to slow down the precipitation and aid to form well defined cube-like AgX^{39, 57} nanostructures due to its high viscosity, about one order of magnitude higher than that of water. Moreover, at the elevated temperature the solvent has enough reducing ability to make AgCl partially in situ transform into metallic Ag⁰ domains or clusters, and produce cube-tetrapod morphology Ag/AgX nanocomposites after an Ostwald ripening process.^{39, 58, 59} However, better defined nanostructures of Ag/AgCl can be obtained by realizing oriented attachment with the assistant of external energy inputs. Round triangular pyramid and cube-shaped Ag/AgCl hybrids have been obtained in one step treatment under the assistant of microwave irradiation⁶⁰ and sonication,⁴⁴ respectively. The reducing radicals generated from EG molecules contribute to the reduction of the surface fraction of AgCl. The SEM images of Ag/AgX with various morphologies were shown in the Fig. 1.

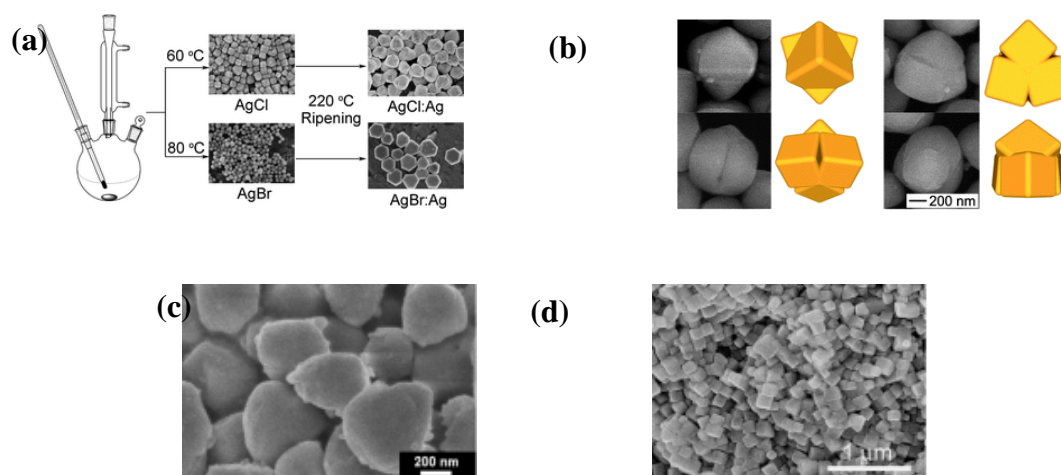


Fig. 1. SEM images of Ag/AgX with various morphologies synthesized in EG solution: (a) Schematic illustration of the synthesis of cube-tetrapod Ag/AgCl and Ag /AgBr nanoplates;⁵⁹ (b) cube-tetrapod Ag/AgCl with a ripening time of 30 min and their corresponding schematic drawings;⁵⁸ (c) triangular pyramids AgCl/Ag synthesized at 140 °C for 1 min by microwave heating;⁶⁰ (d) Ag/AgCl nanocubes synthesized by sonochemical process: ($[Ag^+] = 0.08 \text{ mol L}^{-1}$,

[PVP]=25 g L⁻¹, sonication time=30 min).⁴⁴ Reproduced with permission from Ref. 44, 58, 59 and 60.

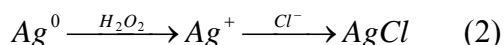
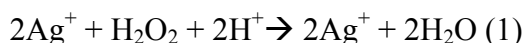
Ionic liquids has been widely used as green solvents, templates, stabilizers, reactants or reaction medium for the synthesis of morphology tunable nanomaterials. Most of ionic liquids have 1-3 orders of magnitude higher viscosity than traditional solvents.⁶¹ Simultaneously, the halogen containing ionic liquids can be involved in the reaction of AgX formation, and the reducing ability of ionic liquids makes the generation of Ag⁰ possible. A hydrothermal method was developed to produce Ag/AgX (X=Cl, Br) nanocomposite in one pot by employing the ionic liquids 1-octyl-3-methylimidazolium chloride ([Omim]Cl)⁴⁶ and 1-hexadecyl-3-methylimidazolium bromide ([C₁₆mim]Br)⁶² as both the precursor and the reducing reagent.

Retarded reaction and morphology controllable for AgX could also be obtained by selecting suitable precursors. With silver acetate and NaCl as the precursors, a template-free direct precipitation method was developed to synthesize cube-like Ag/AgCl nanostructures, in which silver acetate is served as both the silver source and the reductant.⁶³ On the other hand, besides the Cl or Br containing ionic liquid or cation surfactant, other chloride solvent can also be employed as the suitable source. Considering CH₂Cl₂ is a slow release chloride ion source, Han et al. has proposed a solvothermal method with CH₂Cl₂ to produce micrometer cube-like AgCl, which was followed with a post photoreduction to obtain Ag/AgCl.⁶⁴

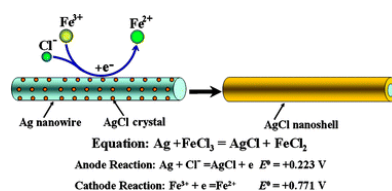
Due to their low solubility, AgX compounds can be easily obtained by an ion exchange process between X⁻ ions and other silver compound precursors, which have relatively higher solubility but can be prepared with better controllable size, morphology and higher purity. Ag₂MoO₄ with various nano-morphologies is frequently used as the precursor for the synthesis of AgCl¹⁵ or AgBr⁶⁵. AgCl nanowires can be obtained by an ion exchange from the silver molybdate nanowires, which are synthesized by a simple precipitation between Ag⁺ and MoO₄²⁻ with tungstosilicic acid as the soft template.⁶⁶ However, the AgCl nanowires would decompose into nanoparticles when transformed into Ag/AgCl by photoreduction.⁶⁶ Ion exchange can also be carried out at solid state. Hu et al. has developed a one-step solid-state reaction method to conversion AgCO₃ into Ag/AgCl by grounding it with HONH₃Cl at room temperature, in which low valence nitrogen atoms contribute to the

reduction and the formation of metallic Ag.⁶⁷ AgCO₃, an semiconductor compound with a band gap of 2.3 eV, is unstable upon illumination.^{31, 68} However, it is an excellent template for the syntheses of porous or hollow nanoarchitectures, because when performing ion exchange and accompanying with acidic etching, AgCO₃ would transform into other silver compounds accompanying with CO₂ evolution and cavity formation. Hierarchical porous AgCl@Ag was obtained by etching AgCO₃ with NH₄Cl,⁶⁹ and porous Ag-Ag₂S nanotubes was achieved by microwave-assisted hydrothermally treating AgCO₃ nanorods with thioacetamide.⁷⁰ In addition, cation exchange is another possible way to fabricate SSC materials. By treating cubic NaCl with AgNO₃, core-shell NaCl@AgCl cubes can be obtained by the exchange of Ag⁺ and Na⁺, and through PR or PAR method, the precursor cubes would transform into Ag/AgCl cubic cages.⁷¹ Those hollow or porous nanoarchitectures always display better photoactivity because of the reflection-enhanced light harvesting efficiency inside the cavities.⁶⁹⁻⁷¹

The synthesis through an oxidation process from Ag⁰ is another important strategy. Several in situ chemical oxidation methods have been developed to convert silver nanostructures into SSC composites with high activity in photochemical reactions. Li et al. suggested a method for porous Ag/AgCl.⁷² In this method, firstly, nanoporous silver was obtained by dealloying Ag₂₀Al₈₀ alloy foils in NaOH solution; and then it was added into a mixed solution of H₂O₂ and HCl to make Ag⁰ partially transformation into AgCl. Herein, Ag⁰ is a catalyst for H₂O₂ decomposition. However, the presence of Cl⁻ would promote the oxidation half-reaction due to the formation of AgCl (equation 1 and 2).



Silver nanowire can be achieved by reducing AgNO₃ in polyol solution with the presence of PVP at a temperature as high as 160 °C,⁴² while silver microsphere can be prepared by reducing AgNO₃ with ascorbic acid and citric acid.⁷³ Based on these nanostructural Ag, a core-shell Ag/AgCl nanoarchitecture can be fabricated by oxidizing Ag precursors with FeCl₃^{42, 73} or ionic liquid [Bmim]FeCl₄.⁷⁴ According to the redox potentials of $E_{\text{AgCl}/\text{Ag}}^0 = +0.223 \text{ V vs. SHE}$ and $E_{\text{Fe}^{3+}/\text{Fe}^{2+}}^0 = +0.771 \text{ V vs. SHE}$, Ag⁰ at the surface of such nanostructures can be in situ oxidized into AgCl by Fe³⁺, as described in the Scheme 1. Moreover, it was found that by treating Ag



Scheme 1. Schematic illustration of the in situ oxidation process for Ag/AgCl core-shell nanowires.⁴² Reproduced with permission from Ref.42.

precursor with the solution containing X^- anion and other metallic cation M^{n+} , Ag/AgX nanocomposites with various morphologies can be obtained. The structure depends much on the redox potentials of AgX/Ag and metal ions, which influence the oxidation rates of Ag.⁴² Furthermore, commercial Ag foil or plate can be directly used as the precursor. AgBr nanowires was synthesized by treating Ag foil in the solution of $\text{Fe}(\text{NO})_3$, NaBr and PVP, because the potential of AgBr/Ag pair (+0.007 V vs. SHE) is much lower than that of $\text{Fe}^{3+}/\text{Fe}^{2+}$.⁷⁵ AgCl concave cubes that preferentially grow along (111) and (110) directions can be achieved by treating Ag plate in a mixed solution of NaClO_2 , NaCl and citric acid.⁷⁶ With the similar method but using excess Cl^- ions to decrease the surface energy of Ag (111) facets, a 3D AgCl hierarchical superstructure with more exposed high-index facets was obtained.⁷⁷ In addition, silver can also be oxidized by O_2 when forming the format of $[\text{Ag}(\text{NH}_3)]^+$ complex, because the redox potential of O_2/OH^- pair (+0.401 V vs. SHE) is slightly higher than that of $[\text{Ag}(\text{NH}_3)]^+/\text{Ag}$ pair (+0.373 V vs. SHE). Based on this, by treating Ag nanowires with $[\text{Ag}(\text{NH}_3)]^+$ complex and Na_2HPO_4 , a necklace-like nanoheterostructure with submicro-cubes Ag_3PO_4 growth on Ag nanowires was obtained,⁷⁸ and when enough capping agent PVP was added in the solution, core-shell coaxial $\text{Ag}_3\text{PO}_4/\text{Ag}$ hetero-nanowires can be synthesized.⁷⁹ Besides chemical oxidation methods, a electrochemical anodic oxidation method was developed by Huang's group.⁸⁰ With the bulk Ag sheet as the anode and $\text{NaCl}+\text{Na}_2\text{SO}_4$ solution as the electrolyte, by adjusting the voltage and the concentration of electrolyte, uniform AgCl nanocubes can be controllably synthesized according to an interface kinetic-diffusion reaction mechanism.⁸⁰

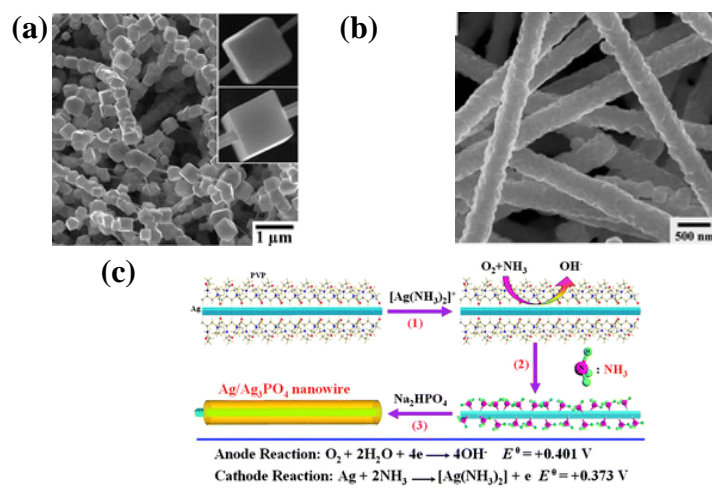
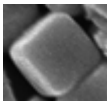
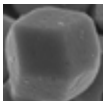
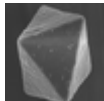
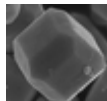
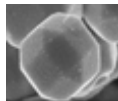


Fig. 2. Necklace-like nanoheterostructure⁷⁸ and core-shell coaxial Ag_3PO_4/Ag ,⁷⁹ Schematic illustrations of the growth process of Ag/Ag_3PO_4 core-shell hetero-nanowires.⁷⁹ Reproduced with permission from Ref. 78 and 79.

It has been found that high energy facets possess higher activity in catalytic reactions and the synthesis of (001) facets dominant anatase TiO_2 becomes a popular strategy for high performance TiO_2 .⁸¹ However, the synthesis of nanomaterials with dominant high energy facets is a challenge due to the instability of these facets, especially for silver compounds. There are only a few studies on this. Through an ionic liquid assisted hydrothermal method, Lou et al. investigated the role of ionic liquids as the oriented growth regulators, and found that the length of the $[C_xmim]Cl$ alkyl chains has a great influence on the morphology of as-synthesized $AgCl$. With longer alkyl chains (C12 and C16), near-spherical $AgCl$ nanoparticles with exposed (001) facets was formed, which showed higher activity than the traditional (100) exposed cubic $AgCl$ nanocrystal.⁸² By controlling the growth of Ag_2O microcrystal with various complexing agents, Wang et al. synthesized single facet exposed Ag_2O microcrystals, including (100) cubes, (110) rhombic dodecahedra and (111) octahedral, in which the first one showed the best photocatalytic activity due to the highest surface energy of the (100) facet.⁸³ The Ag_2O morphology-dependent photocatalytic activity of methyl orange degradation rate was show in Table 2.⁸³ Moreover, $AgBr$ with various dominated facets can be synthesized in dimethyl sulfoxide solution at various temperature, and it was found that the completely (111) bound $AgBr$ octahedra showed the highest photocatalytic activities.⁸⁴ In addition, $AgBr$ nanoplates or polyhedrons possessing increased percentage of (111) facets exposure and displaying enhanced photocatalytic performances can be synthesized by precipitating $AgBr$ in EG

solution with PVP as the capping agent.^{85, 86} Although the studies on the exposure of high energy facets and the control of crystal morphology have made great progress⁸²⁻⁸⁷, the underlying mechanism is still requires much more efforts. According to a recent theoretic study by Ma et al., the surface energies, adsorption energy and total energy for different surfaces upon adsorption of Cl in AgCl were compared, and these provided important intrinsic information to understand the tunable growth of AgX crystal, which can be experimentally achieved by adjusting the concentration of halogen ions.⁸⁸

Table 2 Degradation rate of samples with different morphologies (RD = Rhombic dodecahedra, RB = rhombicuboctahedra, 18 faces = polyhedra with 18 faces).⁸³ Reproduced with permission from Ref.⁸³.

Morphology					
Name	Cubic	RD	Octahedral	18 faces	RB
Degradation rate (10 min)	90%	40%	21%	72%	78%

According to above strategies, beside the most frequently investigated AgX, Ag₂O, Ag₂CO₃ and Ag₃PO₄, other silver compounds, such as Ag₃VO₄,⁸⁹ Ag₂S,^{28, 29, 70} Ag₂Mo₃O₁₀,⁹⁰ Ag₂MoO₄,³³ Ag₂CrO₄,^{91, 92} Ag₂SiO₃ and Ag₉(SiO₄)₂NO₃,²⁰ silver containing polyoxometalate,⁹²⁻⁹⁴ and the corresponding SSC composites have been developed. According to a comparison study by Huang et al., the photocatalytic ability of SSC depends much on the negative charged ions, that is, higher stability and larger charged anions resulting in a better photocatalytic performance.⁹² A comparison study between these SSC materials could offer abundant implications on the relationship on the crystal structure-dependent photochemical performance.

2.2 Multi-component SSC (MSSC) composites

To further improve the activity and stability, a large number of multi-component SSC composites with diverse structures and properties have been studied. Immobilizing SSC composites over a substrate is the most commonly used method. The substrate could be a chemical stable photo-inert material with a large surface area, such as mesoporous silica (MCM-41^{13, 95, 95} and

SBA-15⁹⁶), carbon materials (carbon nanotube,^{24, 97-99} active carbon^{100, 101} and graphene or reduced graphene oxide (RGO)^{55, 21, 102-117} ¹⁰⁰⁻¹¹⁶), ordered mesoporous γ -Al₂O₃,¹¹⁸⁻¹²³ layered double hydroxide (LDH),^{124,125} clay^{126, 127} or other materials.¹²⁸⁻¹³¹ The substrate could also be an efficient semiconductor photocatalyst with any morphologies, including TiO₂,^{11, 16, 17, 51-53, 11, 132-150} WO₃,¹⁵¹⁻¹⁵⁵ Bi₂WO₆,^{156, 157} Bi₂MoO₆,¹⁵⁸ Bi₂₀TiO₃₂,¹⁵⁹ BiVO₄,⁹⁶ ZnO,^{22, 160-163} γ -TaON,¹⁶⁴ layered compound K₄Nb₆O₁₇,^{165, 166} g-C₃N₄,¹⁶⁷⁻¹⁶⁹ BiOX,^{26, 170-176} W₁₈O₄₉,^{177, 178} and so on. Main functions of these substrates include providing high surface area and assisting dispersion, facilitating photogenerated charge separation or electron transportation, enwrapping or covalent bonding SSC to improve their stability, or simultaneously serving as capping reagent to regulating the growth of silver compounds.

Normally, most of MSSC composites can be obtained by employing the as-prepared substrate in the growth of silver or silver compound following with the same methods as the syntheses of TSSC. When the substrate is characterized as two dimensional structure, such as the films of self-organized TiO₂ nanotubes, nanoporous or nanorods,^{133,148} or cotton fabric,^{131, 149} the growth of silver compounds over the surface or inside the nanotubes can be achieved by a facile sequential chemical bath deposition. When the substrates is characterized as layer structures, such as LDH^{124, 125} or K₄Nb₆O₁₇,^{165, 166} which always possess excellent ion-exchange ability, the cations in the substrates can be directly utilized for the formation of silver compounds with the addition of Ag⁺, or Ag⁺ can be inserted into the substrate by a facile ion-exchange process and then followed with the deposition of silver compounds.

Furthermore, by combining with various strategies such as heterojunction, solid solution and Z-scheme design, MSSC composites with more delicate nanoarchitectures and better performance can be developed. Ag/AgX/BiOX (X=Cl, Br and I) is an interesting type of MSSC composites with improved activity, which can be facily synthesized via a one-pot coprecipitation method with the same halide as the source.^{26, 171, 176} Moreover, it was found that the composites obtained by an in situ ion exchange reaction between AgNO₃ and BiOX displayed enhanced photocatalytic performance, and this was attributed to the smaller sizes of AgX.^{170, 172} Ion-exchange is also an effective approach to synthesize hetero-structure of multiple silver compounds, such as the heterojunctions of (AgX/Ag₃PO₄)/(Ag)^{179, 180} and Ag@(Ag₂S/Ag₃PO₄),¹⁸¹ the solid solutions like Ag–AgCl_{1-x}Br_x¹⁸² or the Z-scheme structure like AgI/Ag/AgBr.¹⁸³ Ag₃PO₄ is slightly soluble in aqueous solution (0.02 g L⁻¹).¹⁷⁹ By an ion exchange reaction between the as-prepared rhombic dodecahedral Ag₃PO₄ crystal

and sodium halide, AgX/Ag₃PO₄ core-shell heterocrystals can be obtained, in which AgBr/Ag₃PO₄ displayed the best activity for photocurrent generation and methyl orange photocatalytic degradation.¹⁷⁹ The presence of AgX nanoshells on the surface not only prevents the dissolution of Ag₃PO₄, but also promotes photogenerated electrons and holes separated to the hetero components at the interface due to their matched band potential offsets.^{179, 184} Recently, a facile phase transformation route by the calcinations of Ag₂CO₃ was proposed to synthesis Ag₂O/Ag₂CO₃ heterojunction, which displayed enhanced activity and stability in the photocatalytic reactions.¹⁸⁵ It could be a possible way to fabricate the composites with silver oxides and other thermo decomposable silver compounds.

The superior electron conductivity of Ag⁰ nanoparticles enables the MSSC composite possibly forming a Z-scheme photocatalytic nanostructure, which is similar to the two-photon process of Z-scheme in the natural photosynthesis of green plants. Fig. 4 shows a conceptual diagram of a Z-scheme photocatalytic system, which consists of two semiconductor components and a redox mediator with matched redox potential.¹⁸⁶ In this system, both of the two components are excited: in one side electrons contribute to hydrogen evolution and holes to the oxidation of the redox mediator, whereas in the other side, holes oxidize water to produce oxygen and electrons induce the reduction of the redox mediator to make it maintain stable in the solution. According to this mechanism, such a Z-scheme system is especially suitable for water splitting, because the separation of oxygen and hydrogen evolution can be carried out on two visible light responsive semiconductors with relatively narrow band gaps. A MSSC composite with components having matched band potentials can be regarded as a solid state Z-scheme, in which silver nanoparticles serve as the redox mediator for electron transfer from the CB of one component to the VB of the other one, as the gold nanoparticles in the three-component nanojunction system of CdS-Au-TiO₂.¹⁸⁷ Therefore electrons and holes can be separated efficiently and electrons and holes maintain better reduction and oxidation power. MSSC photocatalysts such as Ag/AgBr/BiOBr,²⁶ AgI/Ag/AgBr¹⁸³, H₂WO₄·H₂O/Ag/AgCl¹⁸⁸ and Ag-AgCl@ Bi₂₀TiO₃₂,¹⁵⁹ have been reported as Z-scheme system. However, more evidence such as photonic efficiency and the potentials of conduction band and valence band of the corresponding components should be measured to confirm the Z-scheme like structures in these SSC composites.

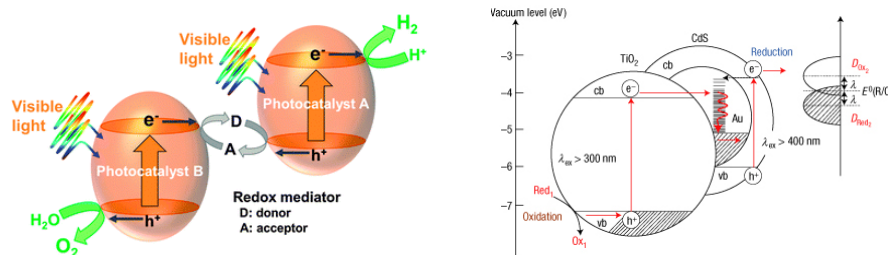


Fig. 3. Conceptual diagram of a Z-scheme photocatalytic system¹⁸⁶ and the energy band diagram scheme of the All-solid-state Z-scheme CdS–Au–TiO₂.¹⁸⁷ Reproduced with permission from Ref. 186 and 187.

3. Electronic structure of SSC composites

There is little basic information on the semiconductor properties (such as p-type, n-type) and parameters (such as band potentials) of silver compounds, which could be attributed to the light sensitive property and impurity of silver compounds under irradiation. It is also one reason for the inconsistent of band gaps obtained from the DRS measurements by different groups. Equation 3 has been proposed to estimate the band potentials of semiconductor oxides, and the estimated data are always acceptable for a comparison.¹⁸⁹ It has also been generalized to estimate the band potentials for all types of silver compounds. However, it should be noted that the comparisons of estimated values could be applicable, but comparing them with the redox potential of chemicals should be avoided. According to this equation, the band potentials of several silver compounds have been calculated in Table 1.

$$E_{CB}^0 = X - E^C - 1/2E_g \quad (3)$$

wherein X is the absolute electronegativity of the semiconductor, expressed as the geometric mean of the absolute electronegativity of the atoms; E^C is the energy of free electrons on the hydrogen scale (~ 4.5 eV); and E_g is the band gap of the semiconductor compound.

First principle calculations based on density functional theory (DFT) is a powerful tool to reveal the origin of the visible light responsive photocatalytic activity of SSC composites. In an earlier study by Calzaferri's group,¹⁹⁰ a self-sensitization mechanism was proposed according to the theoretic calculation of the Ag₁₁₅-(AgCl)₁₉₂ aggregate, in which, the sensitization was attributed to the newly generated metal induced gap states in the energy gap of AgCl and the metal induced d states.¹⁸⁹ However, this mechanism is not clear enough to understand their electronic structure

dependent principle in photochemical reactions and the detailed function of silver nanoparticles. More recently, the photocatalytic performance and stability of Ag/AgCl was revealed through a study on the adsorption of Ag cluster on AgCl surface and the energy transfer at the interface by DFT calculations. The thermodynamic stable structure with the cluster sizes has been understood. It was found that hot holes on Ag cluster can transfer into surface Cl ions producing high oxidative Cl atoms, and more electron-hole pairs can also generated at the interface by the interaction between the plasmonic Ag cluster and the Cl ions.¹⁹¹

The highly dispersive conduction band minimum (CBM) and valence band maximum (VBM) are always beneficial for the transportation of photoexcited electrons and holes, respectively. Theoretic studies on Ag₃PO₄ display that the presence of PO₄ tetrahedral units weakens the covalent nature of Ag-O bonds and inhibits the hybridization of Ag *d* and O *p* orbitals.^{30, 192} Therefore the CBM of Ag₃PO₄ is mainly composed of highly dispersive 5s and 5p bands.^{192, 193} On the other hand, the mobility of carriers is depended much on their effective masses, which can be calculated by fitting parabolic functions to the CBM and VBM along various directions. The effective mass of electrons for TiO₂ is about 1.0 *m_e*.¹⁹⁴ However, most of silver compounds display much smaller effective masses of electrons (~0.6, ~0.6, ~0.4, ~0.25, ~0.18, ~0.15 and ~0.13 *m_e* for Ag₂O, Ag₂SiO₃, Ag₃PO₄, AgCl, AgBr, AgI (wurtzite) and AgI (zinc blende)), which contributes to the high mobility of photoexcited electrons in these compounds.^{20, 192, 195} On the other hand, the structural reasons for the small effective masses of electrons in silver compounds were attributed to the three-dimensional *d*¹⁰-*d*¹⁰ interaction and the relatively short Ag-Ag bonds, which is also advantageous for the reduced band gaps and the dispersion of conduction bands.²⁰ In addition, another reason for the efficient photocatalytic performance of Ag₃PO₄ was ascribed to the inductive effect of PO₄³⁻, that is, the large negative charge and electron cloud overlapping of PO₄³⁻ preferring to attract holes and repel electrons.¹⁹³

It is interesting that SSC composites display exceptional activity for organic degradation under visible light irradiation, even when the wide band gap silver compounds, for example AgCl, do not response visible light. Recently, the plasmon-enhanced photochemical reaction mechanism over the noble metal nanoparticles such as Au, Ag, Cu, has been widely studied.^{196, 197} Although it is still not confirmed the contribution of plasmonic resonance effect of Ag nanoparticles to the photochemical reaction of SSC composites, it was proofed that the injection rate of photoinduced energetic electrons

from Ag nanoparticles to AgCl is very fast, far less than 150 fs according to the transient absorption (TA) spectroscopy measurement; and the electric field near the interface of Ag/AgCl significantly enhanced, as shown in the Figure 5 by an electric field distribution simulation via the 3D finite-difference time-domain (FDTD) method.⁷¹ Anyway, to reveal the detailed mechanism and photochemical processes of such SSC composites is still a big challenge and propelling significant interests.

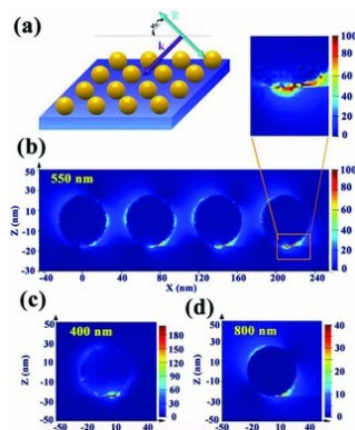


Fig. 4. (a) The simulation model of the 3D FDTD simulation of a 4×4 silver nanospheres array on AgCl substrate excited at 550 nm. (b) Side view of the 3D FDTD simulation result. (c) and (d) Simulation results of electric field distribution for a single silver nanosphere on AgCl substrate at the incident wavelength of 400 nm and 800 nm respectively. The inset in (a) is the large magnification side-view image of the simulation result of (b).⁷¹ Reproduced with permission from Ref.⁷¹.

4. Stability

Although high photocatalytic activity is the ultimate goal for these materials, stability is the priority to ensure them applicable. It is well known that most of silver compounds are light sensitive and prone to decompose into metallic Ag when exposed to light. To maintain the silver compounds stable, the reduction of Ag^+ in the lattice by the photogenerated electrons must be suppressed. This could be achieved by facilitating the transfer of electrons through the introduction of electron scavenger such as AgNO_3 in the reaction solution,³¹ or over the surface such as the Fe(III) cocatalyst.¹⁹⁸ However, the photostability of silver compounds could also be much improved by a self-stable mechanism^{25, 199} or by immobilization on the surface of special oxides such as TiO_2 .²⁰⁰ The self-stabilizing process of Ag_2O has been revealed by Yu et al., as shown in Fig. 5.²⁵ In the first several cycles upon irradiation, the photogenerated electrons on the CB will be captured by the

lattice Ag^+ to form metallic Ag, which is more efficient than the transfer process to oxygen. Then, metallic Ag rapidly formed over Ag_2O surface plays a role of electron sink to facilitate the electron scavenge by oxygen, so as to inhibit the reduction of Ag^+ in the lattice and suppress the further decomposition of Ag_2O .²⁵ A similar self-stabilizing process can be analogized to other silver compounds according to their band potentials. The photodecomposition of silver compounds could also be inhibited when they are immobilized on a semiconductor oxide, such as TiO_2 . It was found that the surface defects of I⁻ vacancy ($\text{Ag}^+ - \text{I}_V^- - \text{Ag}^+$) is the deep electron trap to produce metallic Ag and initiate the decomposition of AgI. However, when immobilized over TiO_2 , the vacancies in AgI are replaced by $\text{Ag}^+ - \text{O}^{2-} - \text{Ti}^{4+}$ bonds on the interface, contributing to a photostable AgI/ TiO_2 composite.²⁰⁰ More efforts still required to understand the photochemical process of SSC composites, and design more stable advanced SSC composites according to the basic mechanistic knowledge.

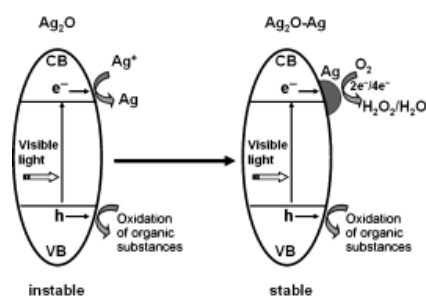


Fig. 5. Schematic diagrams showing the self-stabilizing process of the Ag_2O photocatalyst under fluorescent-light irradiation: left) photogenerated electrons are captured by Ag^+ ions on the as-prepared Ag_2O ; right) photogenerated electrons are captured by O_2 through metallic Ag, which is formed during the initial light irradiation of fresh Ag_2O . (h=holes, e⁻=electrons).²⁵ Reproduced with permission from Ref. 25.

5. Conclusions and outlook

SSC composites have stimulated broad interests in the assembly novel silver compounds based composites for photochemical reactions, and this also provided an opportunity to study of photochemical reactions in a new perspective. In our review, we have introduced the synthetic strategies to tailor the sizes and shapes of SSC nanoarchitectures, summarized the recent advancement on the electronic structure related mechanisms and their stability in the photocatalytic reactions. Although significant enhancement of efficiency has been achieved by tuning the

microstructures and compositions of SSC composites, several challenges in SSC composites are required to be overcome before realizing scalable applicable technology in the near future.

Firstly, to understand the primary photochemical processes in SSC composite requires interdisciplinary knowledge from physics, chemistry, material science, and so on. Although optimistic advances have been achieved on the origination of the enhanced performance of plasmon-enhanced photochemical reactions of metallic nanoparticles,^{195,201} it is still not clear on the relationship between the plasmon-related processes of silver nanoparticles and the photochemical mechanism of the SSC composites. Much more efforts should be taken to build up a comprehensive theoretic scheme to bridge the gaps between photon-related physics and electron-dependent chemistry. The latest progresses on the photon-related physics, such as plasmonic absorption, photon crystal, semiconductor excitation, combining with the current development of the theory calculation methods, should be systematically considered and applied for an in-depth investigation. Secondly, although a large number of SSC composites have been synthesized with enhanced efficiency, it is still urgently demanding to develop industry applicable SSC composites through controllable approaches. To achieve this, not only the efficiency, but also other aspects such as cost and stability should be considered. Stability must be one of the most important factors should be focused on, because in most case silver nanoparticles are susceptible for oxidation, while silver compounds are sensitive to light and decompose to Ag^0 . Moreover the catalysts are always slightly dissoluble in water, making them in particular unstable in the application of aqueous solution. However, this could possibly be figured out by fabricating innovative nanostructures with different metal (Au\Ag\Cu\Al) or constructing smart photochemical systems based on the basic knowledge of SSC composites and the practical situations, including the introduction of electron scavenge center to promote electron transfer, the importation of protection shell layer, the assembly of heterojunctions and photo(electro)catalytic components to regulate the pathway of photogenerated electron-hole pairs, and so on. Finally, due to the great significance of solar fuel, there is still plenty of room for the studies of SSC materials in the capture and conversion of solar energy. Theoretically, high efficiency could also be achieved for water splitting or CO_2 conversion if we can properly regulate the redox potentials of photogenerated charges in the SSC materials. Breakthrough could be made if the questions that how to manipulate the photon-electrons interaction at the interface and how to regulate the multi-photon and multi-electron processes can be answered. It is worth noting that photochemical

conversion of solar energy is a complicate process, and besides above tentatively challenges, much more difficulties will be faced with. However, it can be expected that SSC composites would be at least the brick for gem in this field, and promote the continuous understanding on the primary process in the photochemical reactions.

Acknowledgments

This work is financially supported by National Natural Science Foundation of China (No. 21377084) and Shanghai Municipal Natural Science Foundation (No. 13ZR1421000).

Reference

1. H. Tong, S. Ouyang, Y. Bi, N. Umezawa, M. Oshikiri and J. Ye, *Adv. Mater.*, 2012, **24**, 229-251.
2. F. E. Osterloh, *Chem.Soc. Rev.*, 2013, **42**, 2294-2320.
3. X. Chen, C. Li, M. Gratzel, R. Kostecki and S. S. Mao, *Chem. Soc. Rev.*, 2012, **41**, 7909-7937.
4. A. Kubacka, M. Fernandez-Garcia and G. Colon, *Chem. Rev.*, 2012, **112**, 1555-1614.
5. T. Faunce, S. Styring, M. R. Wasielewski, G. W. Brudvig, A. W. Rutherford, J. Messinger, A. F. Lee, C. L. Hill, H. deGroot, M. Fontecave, D. R. MacFarlane, B. Hankamer, D. G. Nocera, D. M. Tiede, H. Dau, W. Hillier, L. Wang and R. Amal, *Energy Environ. Sci.*, 2013, **6**, 1074-1076.
6. M. C. Long and W. M. Cai, in *Handbook of Photocatalysts: Preparation, Structure and Applications*, G. Castello, Nova Science Pub Inc., New York, 2009, Ch. 8, 297-322.
7. M. Ashokkumar and J. L. Marignier, *Int. J. Hydrog. Energy*, 1999, **24**, 17-20.
8. N. Kakuta, N. Goto, H. Ohkita and T. Mizushima, *J. Phys. Chem. B*, 1999, **103**, 5917-5919.
9. S. Glaus and G. Calzaferri, *J. Phys. Chem. B*, 1999, **103**, 5622-5630.
10. C. Hu, X. X. Hu, L. S. Wang, J. H. Qu and A. M. Wang, *Environ. Sci. Technol.*, 2006, **40**, 7903-7907.
11. Y. H. Zhang, Z. R. Tang, X. Z. Fu and Y. J. Xu, *Appl. Catal. B-Environ.*, 2011, **106**, 445-452.
12. M. Andersson, H. Birkedal, N. R. Franklin, T. Ostomel, S. Boettcher, A. E. C. Palmqvist and G. D. Stucky, *Chem. Mater.*, 2005, **17**, 1409-1415.
13. S. Rodrigues, S. Uma, I. N. Martyanov and K. J. Klabunde, *J. Catal.*, 2005, **233**, 405-410.
14. Y. Li, H. Zhang, Z. Guo, J. Han, X. Zhao, Q. Zhao and a. S.-J. Kim, *Langmuir*, 2008, **24**, 8351-8357.
15. P. Wang, B. Huang, X. Qin, X. Zhang, Y. Dai, J. Wei and M.-H. Whangbo, *Angew. Chem. Int. Ed.*, 2008, **47**, 7931-7933.
16. C. Hu, Y. Q. Lan, J. H. Qu, X. X. Hu and A. M. Wang, *J. Phys. Chem. B*, 2006, **110**, 4066-4072.
17. M. R. Elahifard, S. Rahimnejad, S. Haghghi and M. R. Gholami, *J. Am. Chem. Soc.*, 2007, **129**, 9552-9553.
18. C. Hu, J. Guo, J. Qu and X. Hu, *Langmuir*, 2007, **23**, 4982-4987.
19. D. Schuerch, A. Currao, S. Sarkar, G. Hodes and G. Calzaferri, *J. Phys. Chem. B*, 2002, **106**, 12764-12775.
20. T. G. Kim, D. H. Yeon, T. Kim, J. Lee and S. J. Im, *Appl. Phys. Lett.*, 2013, **103**, 043904.

21. Y. Hou, F. Zuo, Q. Ma, C. Wang, L. Bartels and P. Y. Feng, *J. Phys. Chem. C*, 2012, **116**, 20132-20139.
22. Y. G. Lin, Y. K. Hsu, Y. C. Chen, S. B. Wang, J. T. Miller, L. C. Chen and K. H. Chen, *Energy Environ. Sci.*, 2012, **5**, 8917-8922.
23. M. Abou Asi, C. He, M. H. Su, D. H. Xia, L. Lin, H. Q. Deng, Y. Xiong, R. L. Qiu and X. Z. Li, *Catal. Today*, 2011, **175**, 256-263.
24. M. Abou Asi, L. Zhu, C. He, V. K. Sharma, D. Shu, S. Li, J. Yang and Y. Xiong, *Catal. Today*, 2013, **216**, 268-275.
25. X. Wang, S. Li, H. Yu, J. Yu and S. Liu, *Chem.-Eur. J.*, 2011, **17**, 7777-7780.
26. L. Q. Ye, J. Y. Liu, C. Q. Gong, L. H. Tian, T. Y. Peng and L. Zan, *ACS Catal.*, 2012, **2**, 1677-1683.
27. S. Chen, T. Ida and K. Kimura, *J. Phys. Chem. B*, 1998, **102**, 6169-6176.
28. M. L. Pang, J. Y. Hu and H. C. Zeng, *J. Am. Chem. Soc.*, 2010, **132**, 10771-10785.
29. F. R. Jiang, Q. W. Tian, M. H. Tang, Z. G. Chen, J. M. Yang and J. Q. Hu, *Crystengcomm*, 2011, **13**, 7189-7193.
30. Z. Yi, J. Ye, N. Kikugawa, T. Kako, S. Ouyang, H. Stuart-Williams, H. Yang, J. Cao, W. Luo, Z. Li, Y. Liu and R. L. Withers, *Nat. Mater.*, 2010, **9**, 559-564.
31. G. Dai, J. Yu and G. Liu, *J. Phys. Chem. C*, 2012, **116**, 15519-15524.
32. S. Ouyang, Z. Li, Z. Ouyang, T. Yu, J. Ye and Z. Zou, *J. Phys. Chem. C*, 2008, **112**, 3134-3141.
33. Z. Q. Li, X. T. Chen and Z. L. Xue, *Sci. China-Chem.*, 2013, **56**, 443-450.
34. Q. Zhu, W. S. Wang, L. Lin, G. Q. Gao, H. L. Guo, H. Du and A. W. Xu, *J. Phys. Chem. C*, 2013, **117**, 5894-5900.
35. C. H. An, R. P. Wang, S. T. Wang and X. Y. Zhang, *J. Mater. Chem.*, 2011, **21**, 11532-11536.
36. J. Song, J. Roh, I. Lee and J. Jang, *Dalton Trans.*, 2013, **42**, 13897-13904.
37. J. Song, I. Lee, J. Roh and J. Jang, *Rsc Adv.*, 2014, **4**, 4558-4563.
38. J. H. Kou and R. S. Varma, *Chemsuschem*, 2012, **5**, 2435-2441.
39. C. An, S. Peng and Y. Sun, *Adv. Mater.*, 2010, **22**, 2570-2574.
40. K. Dai, L. H. Lu, J. Dong, Z. Y. Ji, G. P. Zhu, Q. Z. Liu, Z. L. Liu, Y. X. Zhang, D. P. Li and C. H. Liang, *Dalton Trans.*, 2013, **42**, 4657-4662.
41. Z. C. Wang, J. H. Liu and W. Chen, *Dalton Trans.*, 2012, **41**, 4866-4870.
42. Y. Bi and J. Ye, *Chem. Commun.*, 2009, 6551-6553.
43. X. Xu, X. P. Shen, H. Zhou, D. Z. Qiu, G. X. Zhu and K. M. Chen, *Appl. Catal. A-Gen.*, 2013, **455**, 183-192.
44. D. L. Chen, S. H. Yoo, Q. S. Huang, G. Ali and S. O. Cho, *Chem. Eur. J.*, 2012, **18**, 5192-5200.
45. Y. P. Liu, L. Fang, H. D. Lu, Y. W. Li, C. Z. Hu and H. G. Yu, *Appl. Catal. B-Environ.*, 2012, **115**, 245-252.
46. H. Xu, H. Li, J. Xia, S. Yin, Z. Luo, L. Liu and L. Xu, *ACS Appl. Mater. Interfaces*, 2011, **3**, 22-29.
47. M. Choi, K. H. Shin and J. Jang, *J. Colloid Interface Sci.*, 2010, **341**, 83-87.
48. L. H. Dong, D. D. Liang and R. C. Gong, *Eur. J. Inorg. Chem.*, 2012, 3200-3208.
49. M. S. Zhu, P. L. Chen and M. H. Liu, *J. Mater. Chem.*, 2011, **21**, 16413-16419.
50. L. Kuai, B. Y. Geng, X. T. Chen, Y. Y. Zhao and Y. C. Luo, *Langmuir*, 2010, **26**, 18723-18727.
51. D. S. Wang, Y. D. Duan, Q. Z. Luo, X. Y. Li, J. An, L. L. Bao and L. Shi, *J. Mater. Chem.*, 2012, **22**, 4847-4854.

52. P. H. Wang, Y. X. Tang, Z. L. Dong, Z. Chen and T. T. Lim, *J. Mater. Chem. A*, 2013, **1**, 4718-4727.
53. W. X. Wang, L. Q. Jing, Y. C. Qu, Y. B. Luan, H. G. Fu and Y. C. Xiao, *J. Hazard. Mater.*, 2012, **243**, 169-178.
54. L. H. Dong, S. S. Tang, J. Y. Zhu, P. Y. Zhan, L. F. Zhang and F. W. Tong, *Mater. Lett.*, 2013, **91**, 245-248.
55. M. Zhu, P. Chen and M. Liu, *ACS Nano*, 2011, **5**, 4529-4536.
56. R. F. Dong, B. Z. Tian, C. Y. Zeng, T. Y. Li, T. T. Wang and J. L. Zhang, *J. Phys. Chem. C*, 2013, **117**, 213-220.
57. H. Wang, Y. Li, C. Li, L. He and L. Guo, *Crystengcomm*, 2012, **14**, 7563-7566.
58. S. Peng and Y. G. Sun, *J. Mater. Chem.*, 2011, **21**, 11644-11650.
59. C. H. An, J. Z. Wang, W. Jiang, M. Y. Zhang, X. J. Ming, S. T. Wang and Q. H. Zhang, *Nanoscale*, 2012, **4**, 5646-5650.
60. J. Jiang and L. Z. Zhang, *Chem.-Eur. J.*, 2011, **17**, 3710-3717.
61. S. Zhang, N. Sun, X. He, X. Lu and X. Zhang, *J. Phys. Chem. Ref. Data*, 2006, **35**, 1475-1517.
62. H. Xu, Y. H. Song, L. Liu, H. M. Li, Y. G. Xu, J. X. Xia, X. Y. Wu and S. W. Zhao, *J. Chem. Technol. Biotechnol.*, 2012, **87**, 1626-1633.
63. M. S. Zhu, P. L. Chen, W. H. Ma, B. Lei and M. H. Liu, *ACS Appl. Mater. Interfaces*, 2012, **4**, 6386-6392.
64. L. Han, P. Wang, C. Z. Zhu, Y. M. Zhai and S. J. Dong, *Nanoscale*, 2011, **3**, 2931-2935.
65. P. Wang, B. Huang, X. Zhang, X. Qin, H. Jin, Y. Dai, Z. Wang, J. Wei, J. Zhan, S. Wang, J. Wang and M. H. Whangbo, *Chem.-Eur. J.*, 2009, **15**, 1821-1824.
66. Y. Q. Zhu, H. L. Liu, L. B. Yang and J. H. Liu, *Mater. Res. Bull.*, 2012, **47**, 3452-3458.
67. P. F. Hu and Y. L. Cao, *Dalton Trans.*, 2012, **41**, 8908-8912.
68. H. J. Dong, G. Chen, J. X. Sun, C. M. Li, Y. G. Yu and D. H. Chen, *Appl. Catal. B-Environ.*, 2013, **134**, 46-54.
69. L. H. Ai, C. H. Zhang and J. Jiang, *Appl. Catal. B-Environ.*, 2013, **142**, 744-751.
70. W. L. Yang, L. Zhang, Y. Hu, Y. J. Zhong, H. B. Wu and X. W. Lou, *Angew. Chem. Int. Ed.*, 2012, **51**, 11501-11504.
71. Y. Tang, Z. Jiang, G. Xing, A. Li, P. D. Kanhere, Y. Zhang, T. C. Sum, S. Li, X. Chen, Z. Dong and Z. Chen, *Adv. Funct. Mater.*, 2013, **23**, 2932-2940.
72. Y. Y. Li and Y. Ding, *J. Phys. Chem. C*, 2010, **114**, 3175-3179.
73. B. W. Ma, J. F. Guo, W. L. Dai and K. N. Fan, *Appl. Catal. B-Environ.*, 2013, **130**, 257-263.
74. Y. G. Xu, H. Xu, H. M. Li, J. Yan, J. X. Xia, S. Yin and Q. Zhang, *Colloid Surf. A-Physicochem. Eng. Asp.*, 2013, **416**, 80-85.
75. Y. P. Bi and J. H. Ye, *Chem.-Eur. J.*, 2010, **16**, 10327-10331.
76. Z. Lou, B. Huang, X. Qin, X. Zhang, H. Cheng, Y. Liu, S. Wang, J. Wang and Y. Dai, *Chem. Commun.*, 2012, **48**, 3488-3490.
77. Z. Z. Lou, B. B. A. Huang, X. C. Ma, X. Y. Zhang, X. Y. Qin, Z. Y. Wang, Y. Dai and Y. Y. Liu, *Chem.-Eur. J.*, 2012, **18**, 16090-16096.
78. Y. P. Bi, H. Y. Hu, S. X. Ouyang, Z. B. Jiao, G. X. Lu and J. H. Ye, *J. Mater. Chem.*, 2012, **22**, 14847-14850.
79. H. Y. Hu, Z. B. Jiao, T. Wang, J. H. Ye, G. X. Lu and Y. P. Bi, *J. Mater. Chem. A*, 2013, **1**, 10612-10616.

80. Z. Lou, B. Huang, Z. Wang, X. Qin, X. Zhang, Y. Liu, R. Zhang, Y. Dai and M. H. Whangbo, *Dalton Trans.*, 2013, **42**, 15219-15225
81. S. Liu, J. Yu and M. Jaroniec, *Chem. Mater.*, 2011, **23**, 4085-4093.
82. Z. Z. Lou, B. B. Huang, P. Wang, Z. Y. Wang, X. Y. Qin, X. Y. Zhang, H. F. Cheng, Z. K. Zheng and Y. Dai, *Dalton Trans.*, 2011, **40**, 4104-4110.
83. G. Wang, X. C. Ma, B. B. Huang, H. F. Cheng, Z. Y. Wang, J. Zhan, X. Y. Qin, X. Y. Zhang and Y. Dai, *J. Mater. Chem.*, 2012, **22**, 21189-21194.
84. H. Wang, J. T. Yang, X. L. Li, H. Z. Zhang, J. H. Li and L. Guo, *Small*, 2012, **8**, 2802-2806.
85. H. Wang, J. Gao, T. Q. Guo, R. M. Wang, L. Guo, Y. Liu and J. H. Li, *Chem. Commun.*, 2012, **48**, 275-277.
86. H. Wang, X. Lang, J. Gao, W. Liu, D. Wu, Y. Wu, L. Guo and J. Li, *Chem.-Eur. J.*, 2012, **18**, 4620-4626.
87. P. Hu, X. L. Hu, C. J. Chen, D. F. Hou and Y. H. Huang, *Crystengcomm*, 2014, **16**, 649-653.
88. X. C. Ma, Y. Dai, J. B. Lu, M. Guo and B. B. Huang, *J. Phys. Chem. C*, 2012, **116**, 19372-19378.
89. G. Wang, Y. Ren, G. J. Zhou, J. P. Wang, H. F. Cheng, Z. Y. Wang, J. Zhan, B. B. Huang and M. H. Jiang, *Surf. Coat. Technol.*, 2013, **228**, S283-S286.
90. K. Hakouk, P. Deniard, L. Lajaunie, C. Guillot-Deudon, S. Harel, Z. Y. Wang, B. B. Huang, H. J. Koo, M. H. Whangbo, S. Jobic and R. Dessapt, *Inorg. Chem.*, 2013, **52**, 6440-6449.
91. F. Soofivand, F. Mohandes and M. Salavati-Niasari, *Mater. Res. Bull.*, 2013, **48**, 2084-2094.
92. H. Huang, X. Li, Z. Kang, Y. Liu, H. Li, X. He, S. Lian, J. Liu and S.-T. Lee, *Dalton Trans.*, 2010, **39**, 10593-10597.
93. W. H. Zhou, M. H. Cao, N. Li, S. Y. Su, X. Y. Zhao, J. Q. Wang, X. H. Li and C. W. Hu, *Mater. Res. Bull.*, 2013, **48**, 2308-2316.
94. W. H. Zhou, M. H. Cao, S. Y. Su, N. Li, X. Y. Zhao, J. Q. Wang, X. H. Li and C. W. Hu, *J. Mol. Catal. A-Chem.*, 2013, **371**, 70-76.
95. A. Pourahmad, S. Sohrabnezhad and E. Kashefian, *Spectroc. Acta Pt. A-Molec. Biomolec. Spectr.*, 2010, **77**, 1108-1114.
96. Z. J. Zhou, M. C. Long, W. M. Cai and J. Cai, *J. Mol. Catal. A-Chem.*, 2012, **353**, 22-28.
97. Y. G. Xu, H. Xu, J. Yan, H. M. Li, L. Y. Huang, Q. Zhang, C. J. Huang and H. L. Wan, *Phys. Chem. Chem. Phys.*, 2013, **15**, 5821-5830.
98. W. Y. Zhai, G. P. Li, P. Yu, L. F. Yang and L. Q. Mao, *J. Phys. Chem. C*, 2013, **117**, 15183-15191.
99. H. X. Shi, J. Y. Chen, G. Y. Li, X. Nie, H. J. Zhao, P. K. Wong and T. C. An, *ACS Appl. Mater. Interfaces*, 2013, **5**, 6959-6967.
100. J. G. McEvoy, D. A. Bilodeau, W. Q. Cui and Z. S. Zhang, *J. Photochem. Photobiol. A-Chem.*, 2013, **267**, 25-34.
101. J. G. McEvoy, W. Q. Cui and Z. S. Zhang, *Appl. Catal. B-Environ.*, 2014, **144**, 702-712.
102. G. Q. Luo, X. J. Jiang, M. J. Li, Q. Shen, L. M. Zhang and H. G. Yu, *ACS Appl. Mater. Interfaces*, 2013, **5**, 2161-2168.
103. X. F. Yang, H. Y. Cui, Y. Li, J. L. Qin, R. X. Zhang and H. Tang, *ACS Catal.*, 2013, **3**, 363-369.
104. L. Liu, J. C. Liu and D. D. Sun, *Catal. Sci. Technol.*, 2012, **2**, 2525-2532.
105. B. J. Jiang, Y. H. Wang, J. Q. Wang, C. G. Tian, W. J. Li, Q. M. Feng, Q. J. Pan and H. G. Fu, *Chemcatchem*, 2013, **5**, 1359-1367.
106. C. Y. Zeng, M. Guo, B. Z. Tian and J. L. Zhang, *Chem. Phys. Lett.*, 2013, **575**, 81-85.

107. Y. Q. Wang and B. Fugetsu, *Chem. Lett.*, 2013, **42**, 438-440.
108. H. Zhang, X. F. Fan, X. Quan, S. Chen and H. T. Yu, *Environ. Sci. Technol.*, 2011, **45**, 5731-5736.
109. S. Bai, X. P. Shen, H. W. Lv, G. X. Zhu, C. L. L. Bao and Y. X. Shan, *J. Colloid Interface Sci.*, 2013, **405**, 1-9.
110. M. S. Zhu, P. L. Chen and M. H. Liu, *J. Mater. Chem.*, 2012, **22**, 21487-21494.
111. C. Xu, Y. Yuan, A. J. Cui and R. S. Yuan, *J. Mater. Chem.*, 2013, **48**, 967-973.
112. M. S. Zhu, P. L. Chen and M. H. Liu, *Langmuir*, 2012, **28**, 3385-3390.
113. M. S. Zhu, P. L. Chen and M. H. Liu, *Langmuir*, 2013, **29**, 9259-9268.
114. H. Y. Cui, X. F. Yang, Q. X. Gao, H. Liu, Y. Li, H. Tang, R. X. Zhang, J. L. Qin and X. H. Yan, *Mater. Lett.*, 2013, **93**, 28-31.
115. X. H. Meng, X. Shao, H. Y. Li, J. Yin, J. Wang, F. Z. Liu, X. H. Liu, M. Wang and H. L. Zhong, *Mater. Lett.*, 2013, **105**, 162-165.
116. G. Y. He, M. G. Qian, X. Q. Sun, Q. Chen, X. Wang and H. Q. Chen, *Powder Technol.*, 2013, **246**, 278-283.
117. Y. L. Min, G. Q. He, Q. J. Xu and Y. C. Chen, *J. Mater. Chem. A*, 2014, **2**, 1294-1301.
118. Y. Yamashita, N. Aoyama, N. Takezawa and K. Yoshida, *Environ. Sci. Technol.*, 2000, **34**, 5211-5214.
119. X. F. Zhou, C. Hu, X. X. Hu, T. W. Peng and J. H. Qu, *J. Phys. Chem. C*, 2010, **114**, 2746-2750.
120. Y. Y. Zhao, L. Kuai and B. Y. Geng, *Catal. Sci. Technol.*, 2012, **2**, 1269-1274.
121. X. F. Zhou, C. Hu, X. X. Hu and T. W. Peng, *J. Hazard. Mater.*, 2012, **219**, 276-282.
122. C. Hu, T. Peng, X. Hu, Y. Nie, X. Zhou, J. Qu and H. He, *J. Am. Chem. Soc.*, 2010, **132**, 857-862.
123. T. W. Peng, C. Hu, X. X. Hu, X. F. Zhou and J. H. Qu, *Catal. Lett.*, 2012, **142**, 646-654.
124. H. Fan, J. Y. Zhu, J. C. Sun, S. X. Zhang and S. Y. Ai, *Chem.-Eur. J.*, 2013, **19**, 2523-2530.
125. M. Nocchetti, A. Donnadio, V. Ambrogi, P. Andreani, M. Bastianini, D. Pietrella and L. Latterini, *J. Mater. Chem. B*, 2013, **1**, 2383-2393.
126. Y. Q. Yang and G. K. Zhang, *Appl. Clay Sci.*, 2012, **67-68**, 11-17.
127. Y. Q. Yang, G. K. Zhang and W. Xu, *J. Colloid Interface Sci.*, 2012, **376**, 217-223.
128. S. Sohrabnezhad and A. Rezaei, *Superlattices Microstruct.*, 2013, **55**, 168-179.
129. W. Jiang, J. X. Liu, J. Feng, J. Z. Wang, Y. P. Li and C. H. An, *Chin. J. Inorg. Chem.*, 2013, **29**, 1753-1758.
130. C. G. Liu, Z. F. Lei, Y. N. Yang and Z. Y. Zhang, *Water Res.*, 2013, **47**, 4986-4992.
131. D. Y. Wu and M. C. Long, *ACS Appl. Mater. Interfaces*, 2011, **3**, 4770-4774.
132. J. B. Zhou, Y. Cheng and J. G. Yu, *J. Photochem. Photobio. A-Chem.*, 2011, **223**, 82-87.
133. J. G. Yu, G. P. Dai and B. B. Huang, *J. Phys. Chem. C*, 2009, **113**, 16394-16401.
134. W. T. Liu, D. L. Chen, S. H. Yoo and S. O. Cho, *Nanotechnology*, 2013, **24**, 405706.
135. M. R. Elahifard, S. Rahimnejad, R. Pourbaba, S. Haghighi and M. R. Gholami, *Prog. React. Kinet. Mech.*, 2011, **36**, 38-52.
136. Q. Y. Li, Y. Y. Xing, R. Li, L. L. Zong, X. D. Wang and J. J. Yang, *RSC Adv.*, 2012, **2**, 9781-9785.
137. N. K. Shrestha, M. Yang, I. Paramasivam and P. Schmuki, *Semicond. Sci. Technol.*, 2011, **26**, 092002.

138. X. P. Wang and T. T. Lim, *Water Res.*, 2013, **47**, 4148-4158.
139. L. H. Nie, Y. Hu and W. X. Zhang, *Acta Phys.-Chim. Sin.*, 2012, **28**, 154-160.
140. J. Cao, B. Y. Xu, B. D. Luo, H. L. Lin and S. F. Chen, *Appl. Surf. Sci.*, 2011, **257**, 7083-7089.
141. R. F. Dong, B. Z. Tian, J. L. Zhang, T. T. Wang, Q. S. Tao, S. Y. Bao, F. Yang and C. Y. Zeng, *Catal. Commun.*, 2013, **38**, 16-20.
142. E. H. Wang, S. W. Liu, T. G. Li and L. J. Song, *Chin. J. Inorg. Chem.*, 2011, **27**, 537-541.
143. Y. Hou, X. Y. Li, Q. D. Zhao, G. H. Chen and C. L. Rastor, *Environ. Sci. Technol.*, 2012, **46**, 4042-4050.
144. J. F. Guo, B. W. Ma, A. Y. Yin, K. N. Fan and W. L. Dai, *J. Hazard. Mater.*, 2012, **211**, 77-82.
145. J. H. Seo, W. I. Jeon, U. Dembereldorj, S. Y. Lee and S. W. Joo, *J. Hazard. Mater.*, 2011, **198**, 347-355.
146. Y. Hou, X. Y. Li, Q. D. Zhao, X. Quan and G. H. Chen, *J. Mater. Chem.*, 2011, **21**, 18067-18076.
147. G. H. Tian, Y. J. Chen, H. L. Bao, X. Y. Meng, K. Pan, W. Zhou, C. G. Tian, J. Q. Wang and H. G. Fu, *J. Mater. Chem.*, 2012, **22**, 2081-2088.
148. W. Teng, X. Y. Li, Q. D. Zhao and G. H. Chen, *J. Mater. Chem. A*, 2013, **1**, 9060-9068.
149. D. Y. Wu and M. C. Long, *Surf. Coat. Technol.*, 2011, **206**, 1175-1179.
150. W. G. Fan, S. Jewell, Y. Y. She and M. K. H. Leung, *Phys. Chem. Chem. Phys.*, 2014, **16**, 676-680.
151. R. Adhikari, G. Gyawali, T. Sekino and S. W. Lee, *J. Solid State Chem.*, 2013, **197**, 560-565.
152. B. W. Ma, J. F. Guo, W. L. Dai and K. N. Fan, *Appl. Catal. B-Environ.*, 2012, **123**, 193-199.
153. P. Wang, B. Huang, X. Qin, X. Zhang, Y. Dai and M. H. Whangbo, *Inorg. Chem.*, 2009, **48**, 10697-10702.
154. J. Cao, B. D. Luo, H. L. Lin and S. F. Chen, *J. Hazard. Mater.*, 2011, **190**, 700-706.
155. D. L. Chen, T. Li, Q. Q. Chen, J. B. Gao, B. B. Fan, J. Li, X. J. Li, R. Zhang, J. Sun and L. Gao, *Nanoscale*, 2012, **4**, 5431-5439.
156. L. Zhang, K.-H. Wong, Z. Chen, J. C. Yu, J. Zhao, C. Hu, C.-Y. Chan and P.-K. Wong, *Appl. Catal. A-Gen.* 2009, **363**, 221-229.
157. L. S. Zhang, K. H. Wong, H. Y. Yip, C. Hu, J. C. Yu, C. Y. Chan and P. K. Wong, *Environ. Sci. Technol.*, 2010, **44**, 1392-1398.
158. G. H. Tian, Y. J. Chen, X. Y. Meng, J. Zhou, W. Zhou, K. Pan, C. G. Tian, Z. Y. Ren and H. G. Fu, *Chempluschem*, 2013, **78**, 117-123.
159. J. G. Hou, Z. Wang, C. Yang, L. Zhou, S. Q. Jiao and H. M. Zhu, *J. Phys. Chem. C*, 2013, **117**, 5132-5141.
160. G. Begum, J. Manna and R. K. Rana, *Chem.-Eur. J.*, 2012, **18**, 6847-6853.
161. Y. G. Xu, H. Xu, H. M. Li, J. X. Xia, C. T. Liu and L. Liu, *J. Alloy. Compd.*, 2011, **509**, 3286-3292.
162. Q. Zhang, C. G. Tian, A. P. Wu, Y. Hong, M. X. Li and H. G. Fu, *J. Alloy. Compd.*, 2013, **563**, 269-273.
163. S. M. Lam, J. C. Sin, A. Z. Abdullah and A. R. Mohamed, *Chemical Papers*, 2013, **67**, 1277-1284.
164. J. G. Hou, C. Yang, Z. Wang, Q. H. Ji, Y. T. Li, G. C. Huang, S. Q. Jiao and H. M. Zhu, *Appl.*

- Catal. B-Environ.*, 2013, **142**, 579-589.
165. W. Q. Cui, H. Wang, Y. H. Liang, L. Liu and B. X. Han, *Catal. Commun.*, 2013, **36**, 71-74.
166. W. Cui, H. Wang, L. Liu, Y. Liang and J. G. McEvoy, *Appl. Surf. Sci.*, 2013, **283**, 820-827.
167. H. Xu, J. Yan, Y. G. Xu, Y. H. Song, H. M. Li, J. X. Xia, C. J. Huang and H. L. Wan, *Appl. Catal. B-Environ.*, 2013, **129**, 182-193.
168. Y. H. Lan, X. Z. Qian, C. J. Zhao, Z. M. Zhang, X. Chen and Z. Li, *J. Colloid Interface Sci.*, 2013, **395**, 75-80.
169. J. Cao, Y. J. Zhao, H. L. Lin, B. Y. Xu and S. F. Chen, *Mater. Res. Bulletin*, 2013, **48**, 3873-3880.
170. H. F. Cheng, W. J. Wang, B. B. Huang, Z. Y. Wang, J. Zhan, X. Y. Qin, X. Y. Zhang and Y. Dai, *J. Mater. Chem. A*, 2013, **1**, 7131-7136.
171. H. F. Cheng, B. B. Huang, Y. Dai, X. Y. Qin and X. Y. Zhang, *Langmuir*, 2010, **26**, 6618-6624.
172. H. F. Cheng, B. B. Huang, P. Wang, Z. Y. Wang, Z. Z. Lou, J. P. Wang, X. Y. Qin, X. Y. Zhang and Y. Dai, *Chem. Commun.*, 2011, **47**, 7054-7056.
173. H. L. Lin, J. Cao, B. D. Luo, B. Y. Xu and S. F. Chen, *Chin. Sci. Bull.*, 2012, **57**, 2901-2907.
174. L. Kong, Z. Jiang, H. H. Lai, R. J. Nicholls, T. C. Xiao, M. O. Jones and P. P. Edwards, *J. Catal.*, 2012, **293**, 116-125.
175. C. Cheng, Y. H. Ni, X. Ma and J. M. Hong, *Mater. Lett.*, 2012, **79**, 273-276.
176. W. Xiong, Q. D. Zhao, X. Y. Li and D. K. Zhang, *Catal. Commun.*, 2011, **16**, 229-233.
177. S. B. Sun, X. T. Chang, L. H. Dong, Y. D. Zhang, Z. J. Li and Y. Y. Qiu, *J. Solid State Chem.*, 2011, **184**, 2190-2195.
178. X. T. Chang, S. B. Sun, L. H. Dong and Y. S. Yin, *Mater. Lett.*, 2012, **83**, 133-135.
179. Y. P. Bi, S. X. Ouyang, J. Y. Cao and J. H. Ye, *Phys. Chem. Chem. Phys.*, 2011, **13**, 10071-10075.
180. W. S. Wang, H. Du, R. X. Wang, T. Wen and A. W. Xu, *Nanoscale*, 2013, **5**, 3315-3321.
181. J. T. Tang, W. Gong, T. J. Cai, T. Xie, C. Deng, Z. S. Peng and Q. Deng, *RSC Adv.*, 2013, **3**, 2543-2547.
182. M. S. Zhu, C. C. Chen, P. L. Chen, B. Lei, W. H. Ma and M. H. Liu, *Phys. Chem. Chem. Phys.*, 2013, **15**, 12709-12716.
183. H. L. Lin, J. Cao, B. D. Luo, B. Y. Xu and S. F. Chen, *Catal. Commun.*, 2012, **21**, 91-95.
184. Y. F. Wang, X. L. Li, Y. W. Wang and C. M. Fan, *J. Solid State Chem.*, 2013, **202**, 51-56.
185. C. Yu, G. Li, S. Kumar, K. Yang and R. Jin, *Adv. Mater.*, 2014, **26**, 892-898.
186. Y. Horiuchi, T. Toyao, M. Takeuchi, M. Matsuoka and M. Anpo, *Phys. Chem. Chem. Phys.*, 2013, **15**, 13243-13253.
187. H. Tada, T. Mitsul, T. Kiyonaga, T. Akita and K. Tanaka, *Nat. Mater.* 2006, **5**, 782-786.
188. X. Wang, S. Li, Y. Ma, H. Yu and J. Yu, *J. Phys. Chem. C*, 2011, **115**, 14648-14655.
189. M. A. Butler, D. S. Ginley, *J. Electrochem. Soc.* 1978, **125**, 228-232.
190. S. Glaus, G. Calzaferri and R. Hoffmann, *Chem.-Eur. J.*, 2002, **8**, 1786-1794.
191. X. Ma, Y. Dai, M. Guo, Y. Zhu and B. Huang, *Phys. Chem. Chem. Phys.*, 2013, **15**, 8722-8731.
192. N. Umezawa, O. Shuxin and J. Ye, *Phys. Rev. B*, 2011, **83**, 035202.
193. X. Ma, B. Lu, D. Li, R. Shi, C. Pan and Y. Zhu, *J. Phys. Chem. C*, 2011, **115**, 4680-4687.
194. D. Kurita, S. Ohta, K. Sugiura, H. Ohta and K. Koumoto, *J. Appl. Phys.*, 2006, **100**, 096105.

195. X. C. Ma, Y. Dai, M. Guo and B. B. Huang, *Chemphyschem*, 2012, **13**, 2304-2309.
196. S. Linic, P. Christopher and D. B. Ingram, *Nat. Mater.*, 2011, **10**, 911-921.
197. X. M. Zhang, Y. L. Chen, R. S. Liu and D. P. Tsai, *Rep. Prog. Phys.*, 2013, **76**, 046401.
198. H. G. Yu, L. L. Xu, P. Wang, X. F. Wang and J. G. Yu, *Appl. Catal. B-Environ.*, 2014, **144**, 75-82.
199. H. G. Yu, L. Liu, X. F. Wang, P. Wang, J. G. Yu and Y. H. Wang, *Dalton Trans.*, 2012, **41**, 10405-10411.
200. W. Sun, Y. Z. Li, W. Q. Shi, X. J. Zhao and P. F. Fang, *J. Mater. Chem.*, 2011, **21**, 9263-9270.
201. S. Linic, P. Christopher, H. Xin and A. Marimuthu, *Acc. Chem. Res.*, 2013, **46**, 1890-1899.